Brilliant biophotonics

Wilts, Bodo Dirk

Chapter 1

General Introduction

Since time immemorial, the vivid colours of many animals have mesmerised physicists, biologists and laymen alike [1]. The biological world has exploited photonic structures since the Cambrian explosion over 500 million years ago, with which an enormous diversification of life started. Ever since, the (co-)evolution of prey and predators has led to the amazing diversity of biological organisms present nowadays that make use of different coloration mechanisms to reflect bright colours [2,3].

The most dazzling colours found in animals are the *structural colours* generated by the interaction of light with (quasi-)ordered nanostructured materials, with an order on the mesoscale, ~200 nm [1-5]. These nanostructured materials reside in the outermost parts of the animal integuments, e.g. the feathers of birds, the elytra and scales of beetles and the wing scales of butterflies, so to allow an effective interaction with incoming light.

Structural colours are often *iridescent*, i.e. the colour of the animal's surface changes with the viewing angle. As a consequence of the highly changeable colours, iridescent colours are often described as rainbow-like, metallic, sparkling or opalescent. Actually, striking examples of natural iridescent colours can also be encountered in a whole range of living organisms other than birds, beetles and butterflies: various bacteria, plants and fruits feature strongly iridescent colours [6], but also in non-living materials, such as minerals as opals and shells [7]. On a daily basis, we encounter structural colours in the splendid colours of soap bubbles, but also in the metallic coatings of many electronic devices, e.g. mobile phones.

From a physical point-of-view, the astonishing palette of organismal photonic nanostructures are very effective light control devices and, since also many man-made photonic materials from the 20th and 21st century rely on proper knowledge of light manipulation and control, these biological structures offer an important source for inspiration of technological applications, giving rise to the field of bio-mimicry or bio-mimetics [4,8]. Therefore, a precise interpretation of biological photonic structures often gives rise to the development of new high-tech materials, especially since biological materials often surpass materials generated by present day manufacturing in terms of quality and optical effects. Biological

photonic structures are thus often used as blue-prints for a reproduction of these structures by technological processes [4].

Many studies that were inspired by biological photonic structures have recently led to the birth of various advanced materials, ranging from materials that increase the efficiency of solar cells and (solid-state) lasers [9] to the possible development of all-integrated optical computers [10]. Furthermore, animal colours have also paved the way for high-speed thermal imaging devices [11], highly sensitive gas sensors [12] and better anti-forgery coatings [13].

This thesis focuses on the physical principles underlying animal coloration. In the different chapters of this thesis, various photonic structures on the wing scales of butterflies and weevils, the wings of beetles to the feathers of birds are investigated. The physical principles were revealed in the course of an investigation of the spectral and spatial scattering properties of the animal integuments with a number of physical devices and novel techniques (see **chapter 2**), and compared with detailed computational modelling of the determined nanostructures (see **chapter 3**). Since organismal body colours play an important role in the animal kingdom [3,4,14], our findings are supplemented by a discussion on the possible biological function of the animal's display.

In this introductory chapter, we survey the physical principles of animal coloration. We begin with a treatment of the two main classes of animal coloration: pigmentary and structural coloration. Subsequently, we introduce the concept of (quasi-)ordered photonic crystals and present typical cases. A summary of different biological functions of animal coloration finishes this chapter.

1. Principles of Animal Coloration

Generally, animal coloration results from the reflection of light from an integumental surface. Two main classes of animal coloration exist: *pigmentary coloration*, attributed to the wavelength-selective light absorption by chemical pigments, and *structural coloration*, attributed to the wavelength-selection light reflection due to ordered structures. Both coloration mechanisms feature unique optical properties that will be surveyed and discussed below.

1.1 Pigmentary coloration

This is the most abundant coloration principle found in nature. It is based on the deposition of pigment(s) in the exterior integumental layers and creates most of the yellow, orange, red and brown-black colours observed in nature. Pigmentary coloration is due to the interaction of light with chemical substances that selectively absorb incident light. The pigments are usually immersed throughout randomly ordered structures, that can range from filigree networks to randomly ordered granules as found in many pierid wing scales [15,16], so that incident light, which is not absorbed by the pigment(s), is scattered diffusely. Due to the non-directional nature of this scattered light, pigmentary colours appear identical from all viewing angles and are often described as dull and lustreless.

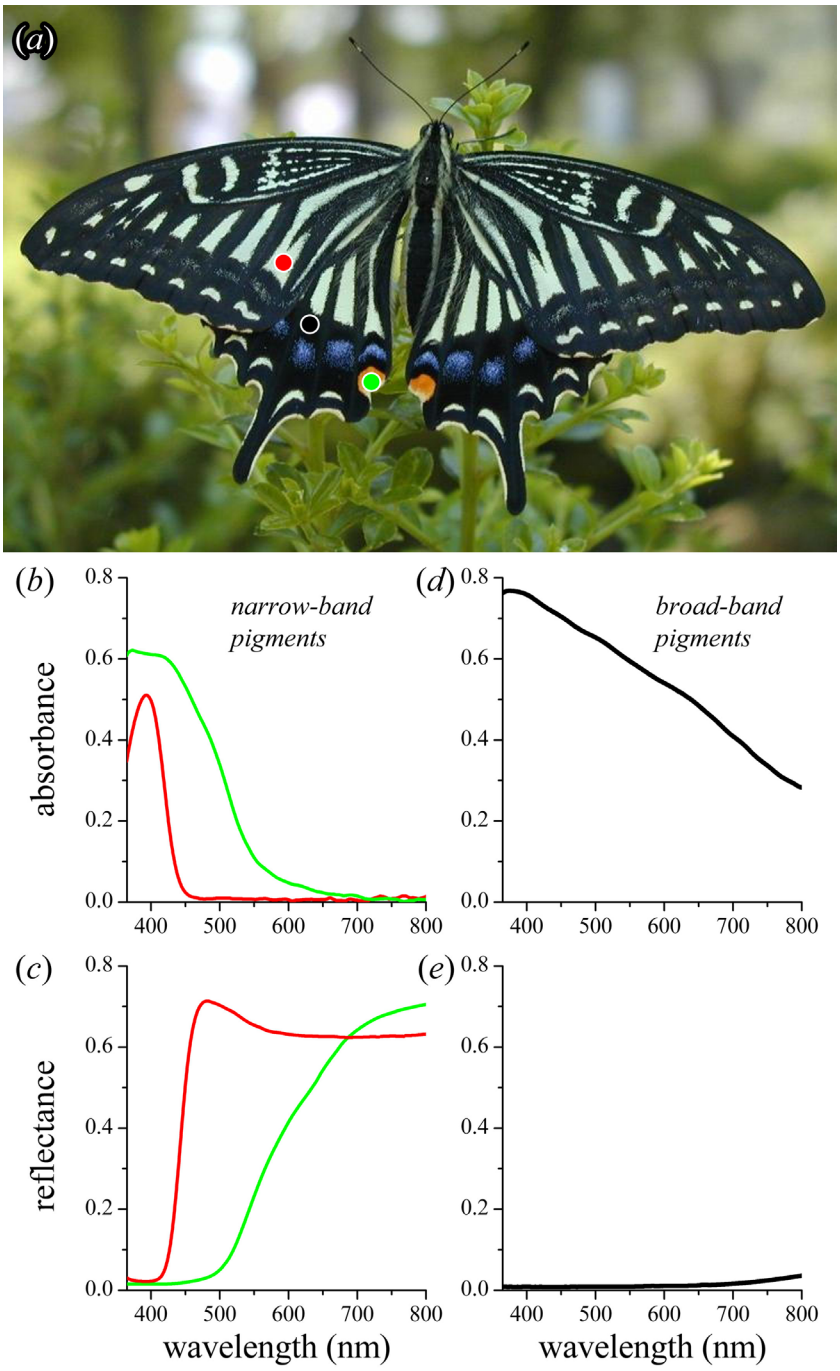

Figure 1. Pigmentary coloration. The dorsal surface of the Asian Swallowtail, *Papilio xuthus* (*a*, photograph by Jani Patokallio), is marked by large areas of yellow, orange and black scales. The yellow and orange wing areas (*b*,*c*) are due to the presence of narrow-band absorbing pigments, resulting in sigmoidal shaped reflectance spectra. The black areas (*d*,*e*) are created by melanin presence in the wing scales. Melanin is a broad-band absorbing pigment that absorbs light in the full visible wavelength range. The blue wing areas are due to structurally coloured wing scales. Coloured spots in (*a*) correspond to measurement areas for spectral measurements (*b*-*e*).

Characteristic for a given pigment is its absorbance spectrum $A(\lambda)$, which often features prominent absorbance bands. Many organic pigments have absorbance bands with a full width at half maximum (FWHM) of ~100 nm and consequently, when deposited in high concentration, these pigments effectively act as *long-pass spectral filters* and create sigmoidal-shaped reflectance spectra. We therefore call pigments with this characteristic spectrum *narrow-band (absorbing) pigments*. Typical examples are the pigments of the yellow- and orange-coloured wing scales of the Asian Swallowtail, *P. xuthus*, the absorbance and reflectance spectra of which are shown in figure 1b,c.

Due to chemical differences, the spectral location of the absorbance bands can substantially differ. Well-studied examples of narrow-band absorbing pigments are the pterin pigments of pierid butterflies: leucopterin, xanthopterin and erythropterin [17]. Leucopterin absorbs exclusively in the UV-wavelength range, thus creating the white (yet UV-dark) colour of the well-known cabbage butterflies, while xanthopterin and erythropterin additionally absorb in the blue- and green-wavelength ranges, therefore creating the yellow, orange or red colours of congeneric pierid butterflies [16-18]. Other narrow-band absorbing pigments include carotenoid, kyunerine and ommochrome pigments, which are expressed in the wing scales of various nymphalid butterflies.

Not all pigments have prominent, narrow absorbance bands. The absorbance spectrum of some pigments, mostly the abundant melanin pigments, eumelanin and pheomelanin, is very broad throughout the full visible wavelength range (up to the near-infrared). Melanin deposition thus underlies most black or brown colours of animal integuments, e.g. the brown and red colours of human hairs, horse skin and bird feathers, but also the brown-black wing scales of papilionid butterflies, like *P. xuthus* (figure 1d,e). We categorise this type of pigments with a broad spectral absorbance as *broad-band (absorbing) pigments*.

1.2 Structural coloration

The most intense and bright colours in nature are due to the interaction of light with regularly ordered, photonic structures resulting in structural colours. To allow (constructive) interference of visible light, photonic structures have to consist of at least two materials having different refractive indices with periodicities of the order on the mesoscale (~200 nm). Photonic structures are often assemblies from dielectric materials with negligible light absorption, such as keratin (bird feathers) or the cuticular chitin (insect cuticle), but also regularly ordered structures of pigmented material can create structural colour, like the melanin layers in bird feathers and beetle elytra.

An important parameter for the reflectance of a photonic structure is the refractive index (RI) contrast of the material components, n_1/n_2. An increase (decrease) of the RI contrast enhances (reduces) the structure's reflectance. In animal photonic structures, an increase of the RI contrast is mostly achieved by replacing a solid, dielectric material with air or by increasing the concentration of a biological pigment, like melanin. This principle of RI contrast increase can for example be observed in the wing scales of the Madagascan Sunset Moth, *Chrysiridia rhipheus*. The wing scale carries assemblies of air-chitin multilayers that create the sparkling colours of the moth [19]. In contrast to that, the wing scales of many lycaenid butterflies carry assemblies of air-chitin multilayers with perforated chitin layers.

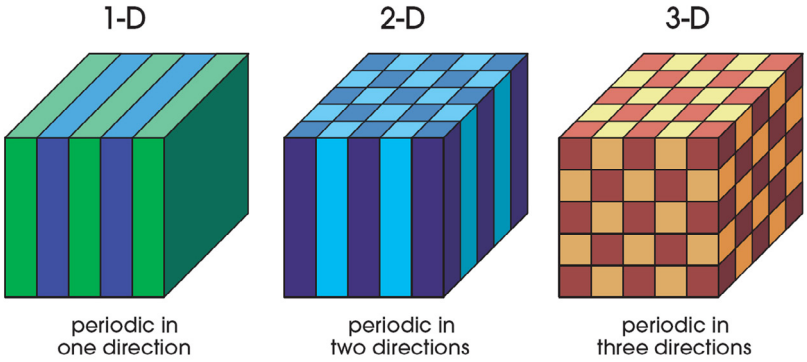

Figure 2. Characterization of photonic structures. Ideal representatives of photonic structures, showing (*a*) one-, (*b*) two- and (*c*) three-dimensional photonic structures made out of two different constituents [5]. The different constituents have to have a different refractive index in order to achieve light interference.

The perforation decreases the RI of the chitin layer and thus the RI contrast, which reduces the reflectance. The perforation however increases the spatial spread of the reflected light [20].

Photonic structures can be most suitably characterised by the number of directions in a three-dimensional Euclidian space in which the photonic structure, i.e. the material constituents and the connected spatial refractive index (RI) distribution $n(\mathbf{r}, \lambda)$, is periodic (figure 2). This gives rise to one-, two- and three-dimensional photonic structures.

Biological photonic structures are of course not *ideal* photonic structures in the way that the structures are not infinitely large. Yet, most photonic structures can be adequately described as 1D, 2D or 3D photonic structures due to their local order and the large domain size compared to the wavelength of visible light. Furthermore, most biological photonic structures show a well-tuned interplay between regularity of the photonic structure and irregularity on different length scales, for example to broaden the visibility range of the reflectance.

In **Chapter 6,** we will further investigate the role of order and disorder in the photonic structure in the wing scales of various papilionid butterflies. We for the first time show that a certain amount of disorder is needed to smooth the reflectance spectrum of a photonic structure.

1.2.1 One-dimensional photonic structures

One-dimensional (1D) photonic structures (figure 2a), such as thin films or multilayers, are probably the most abundant form of structural colouration found in nature, causing the iridescent, metallic colours of many birds, beetles and butterflies. Light reflected by 1D photonic structures is often strongly polarised under high angles of light incidence, which may potentially serve as a visual signal to conspecifics (see below).

The simplest case of a 1D photonic structure is a thin film, i.e. a single layer of material. The most extreme case of a thin film can be found in the clear wings of many flies, but also in the so-called glass scales of the Common Bluebottle, *Graphium sarpedon*, a butterfly native to South and Southeast Asia. The glass scales, that cover large patches of the wing

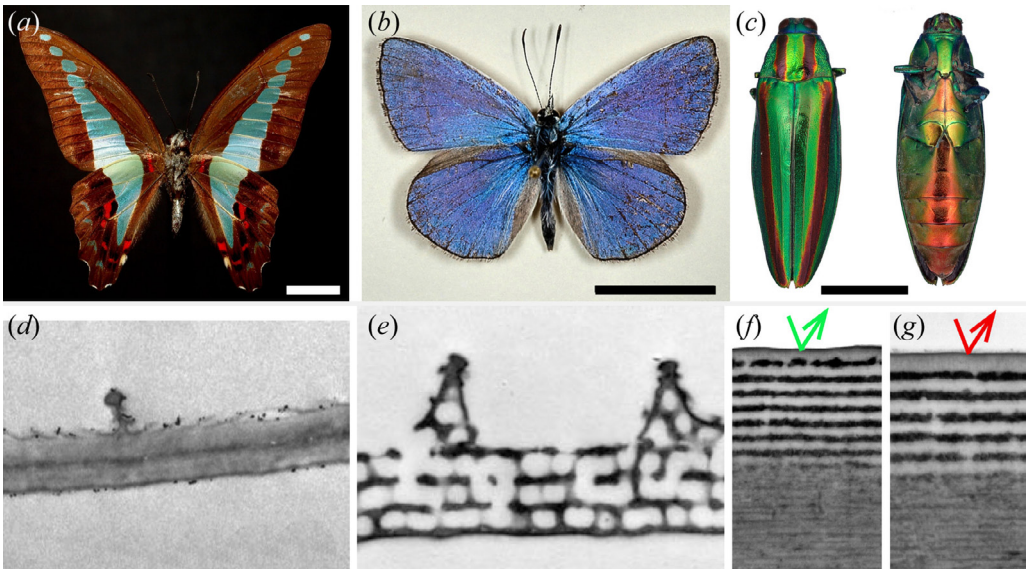

Figure 3: Examples of 1D photonic structures. (*a*,*d*) The glass scales of *G. sarpedon* are formed by a single layer of chitin [21]. (*b*,*e*) Lycaenids have wing scales that carry perforated chitin-air multilayers ([20,22]). (*c*,*f*,*g*) The metallic colors of the Japanese Jewel beetle, *C. fulgidissima*, are due to melanin-chitin multilayer with different dimensions (see **chapter 4**, ref. [23,24]). Bars: (*a*-*c*) 1 cm, (*d*-*g*) 500 nm.

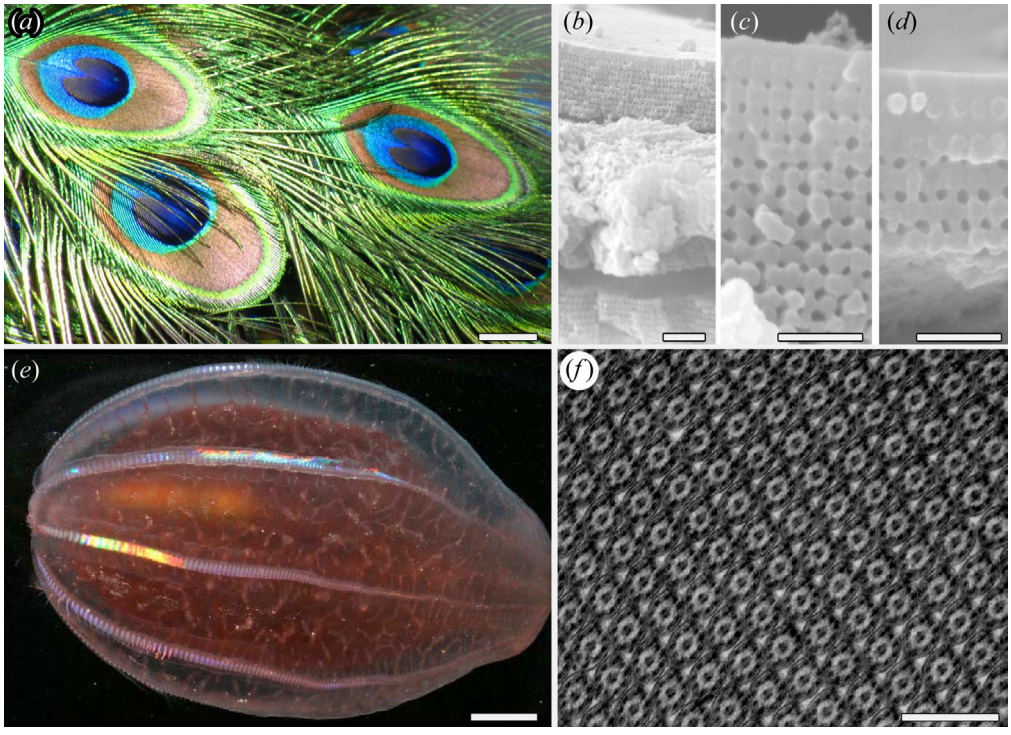

Figure 4: Examples of 2D photonic structures. (*a*-*d*) The photonic structure that underlies the brilliant colors of the eye spots of peacock feathers is a matrix of melanin rodlets in an air environment that is arranged in a square lattice (*b*). Different colours are reflected due to different dimensions and numbers of layers, (*c*) green, (*d*) brown (adapted from [26]). (*e*,*f*) The striking colours of the comb jelly *Beroë cucumis* are due to a 2D lattice of cylinders in the comb rows [27,28]. Bars: (*a*,*e*) 1 cm, (*b*) 1 µm. (*c*,*d*,*f*) 500 nm.

underside, are shaped into a single layer of chitin with a thickness of approx. 400 nm (see figure 3a) [21].

More common 1D photonic structures are multilayer arrangements, i.e. an alternating stacking of thin films with different refractive materials, like the air-chitin multilayers in the wing scales of the Sunset Moth and many lycaenids (figure 3b). In fact, multilayered structures are also used in many technical applications as, for instance, interference filters and anti-reflection coatings [25].

In **Chapter 4,** we investigate the multilayered photonic structures that cause the sparkling, metallic reflections of the elytra of the Japanese Jewel Beetle, *Chrysochroa fulgidissima*, a wood-boring beetle native to Japan (figure 3c). We model the photonic structure with a gradient RI approach that accounts for differences in local order and allows a first estimation of the RI value for melanised chitin.

In **Chapter 5**, we present the first direct measurement of the wavelength-dependent RI of melanin, performed to understand the spectacular reflectance of the occipital nape feather of the bird of paradise, Lawes parotia. Surprisingly, the directional, broad-band silver reflectance is created by a melanin-keratin multilayer that is optimised for reflectance in the near-IR.

1.2.2 Two-dimensional photonic structures

Two-dimensional (2D) photonic structures (see figure 2b) have two periodic directions and are thus essentially made up of locally parallel fibres in a square or hexagonal lattice. To date, relatively few 2D photonic structures have been found in animals.

Striking examples of 2D photonic structures are the eye spots on the tail feathers of the peacock, *Pavo cristatus*. In the feathers, a square lattice of melanin rodlets surrounded by air acts as a 2D photonic structure (figure 4a-d). The diversity of different, iridescent colours in the eyespots arises from a change in the local dimensions and the numbers of melanin layers [26].

Other well-studied examples with 2D photonic structures are the com jelly *Beroë sp.* [27,28] and the polychaete worm *Pherusa sp*. [29]. In these animals, strong photonic effects which arise from an internally close-packed 2D-periodic structure that consists of hollow cylindrical channels, the biological function of which remains unknown (figure 4e,f).

1.2.3 Three-dimensional photonic structures

In three-dimensional (3D) photonic structures, also called *photonic crystals*, all three spatial dimensions have a distinct periodicity (see figure 2c). In general, the unit cell length in the different directions may be unequal. In the animal kingdom, however, all biological 3D photonic crystals determined to date are *cubic* photonic crystals, i.e. with equal unit cell lengths in a Cartesian coordinate system.

Ordered three-dimensional (3D) photonic structures occur in different shapes in butterflies and weevils and usually consist of interconnecting networks of air (RI = 1) and the animal's basic dielectric material, cuticular chitin (RI ~ 1.55, [31]). These material networks can be usually approximated by one of three fundamental bicontinuous cubic structures: primitive cubic (P-surface), diamond (D-surface) or gyroid (G-surface) [30,32,33]. In bicontinuous

cubic structures, the separation between the two material interfaces is defined by an intermaterial dividing surface (IMDS) that can be approximated by level surfaces. For the three fundamental cubic structures, the level surfaces are given by

$$\begin{aligned} \cos X + \cos Y + \cos Z &= t \quad \text{P surface} \\ \cos Z \sin(X+Y) + \sin Z \cos(X-Y) &= t \quad \text{G surface} \\ \sin X \cos Y + \sin Y \cos Z + \cos X \sin Z &= t \quad \text{D surface} \end{aligned} \qquad (1)$$

with the scaled spatial directions X,Y,Z ($X = 2\pi x/a$, etc.), the cubic unit cell size a and the threshold parameter t (see figure 2). From the level surface equations (eq. 1), the RI distribution function $n(x,y,z)$ or the dielectric function $\varepsilon(x,y,z)$ of a photonic crystal can be constructed. This is done by assigning material 1 with RI n_1 for values where $n(x,y,z) < t$ and material 2 with RI n_2 for values where $n(x,y,z) \geq t$. The threshold parameter hence determines the volume fraction f of the two material components, e.g. $t = 0$ gives equal volume fractions, i.e. $f_1 = f_2 = 0.5$, while for $t = -1$ the material fractions in the diamond topology (D) are $f_1 = 0.17$ and $f_2 = 0.83$. The resulting topologies of the photonic crystals are shown in figure 5 for equal material fraction, $t = 0$. From these three structures, the gyroid structure (figure 5c) is unique in that it is intrinsically chiral. The chirality of the photonic crystal network has important consequences for the reflectance of circularly polarised light [34].

Interestingly, the precise topology of 3D photonic crystals in the animal kingdom seems to be restricted to certain orders: while gyroid-type photonic crystals are solely observed in the wing scales of butterflies (Lepidoptera), e.g. in the wing scales of the Green Hairstreak *Callophrys rubi* (figure 6a, refs. [30,35-37]) or the Emerald-patched Cattleheart, *Parides sesostris* (**see chapter 8**), diamond-type photonic crystals seem to be exclusive to weevils (Coleoptera, refs. [4,38-40]); it occurs, e.g. in the wing scales of the diamond weevil *Entimus imperialis* (figure 6b, **see also chapters 9 & 10**). The developmental pathway of the 3D photonic crystals *in vivo* is still unclear, however, it is commonly agreed that cubic membrane folding is a developmental precursor [36,41].

3D photonic crystals can be seen as analogues to semiconductors in electronics, since ranges of light wavelengths exist, where light is forbidden to propagate inside the photonic crystal [5,30,39,43]. In other words, light of this wavelength cannot be transmitted through the crystal and is reflected. Thus, in complete analogy to semiconductors, photonic crystals can also be described by photonic band structure diagrams that may feature *photonic bandgaps* (but see **chapter 3**). A photonic bandgap is called a *complete bandgap* when it exists over all possible orientations of a crystal for any polarisation of incident light; it is called a *partial bandgap* or *pseudogap* when the range of forbidden wavelengths changes with the orientation of the crystal. In biological photonic crystals the RI contrast is usually too low to form complete photonic bandgaps, since a complete bandgap for a diamond-type photonic crystal only opens up for a RI contrast of minimally 2 (**see chapter 9**).

Nevertheless and especially due to the too small RI contrast, biological photonic structures feature a remarkable iridescence. The iridescence of a photonic crystal can be most adequately described by the concept of the first Brillouin zone, which contains the underlying local symmetries of the structure and the characteristic length scales that cause iridescence. In **Chapter 9**, we will for the first time measure the iridescence of a diamond-type 3D biological photonic crystal and show how it is connected to the first Brillouin zone.

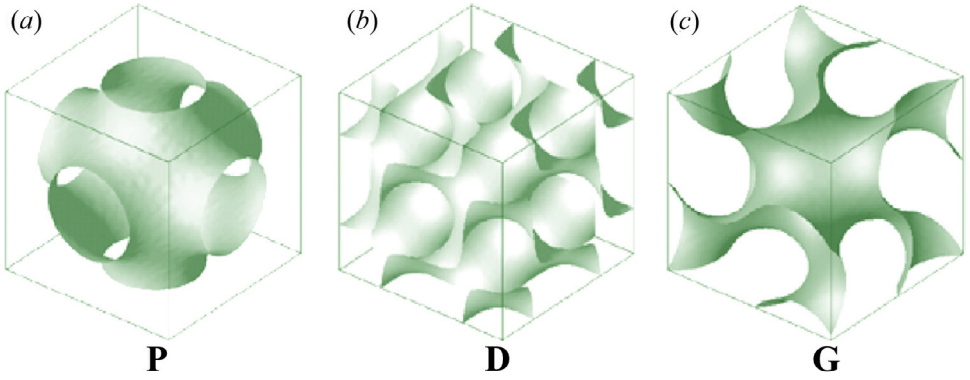

Figure 5: Three-dimensional photonic crystals. Level surfaces of the P-, D- and G-surface constructed from equation 1, with equal material volume fraction, i.e. $t = 0$. These level surfaces divide the cubic structure into two regions of bicontinuous interpenetrating networks (from [30]).

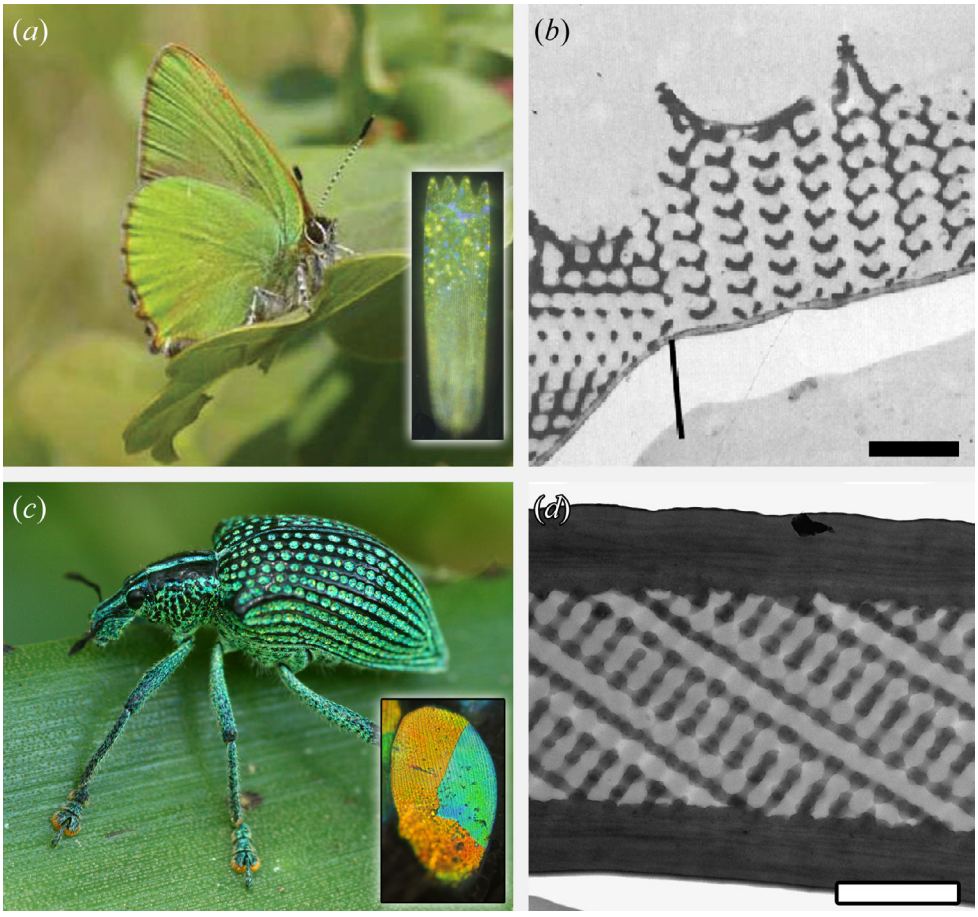

Figure 6: Examples of 3D photonic structures. (*a*,*b*) Gyroid-type photonic crystals in the wing scales of the Green Hairstreak, *C. rubi*, are arranged in small domains on the scales (see inset) and have a chitin filling fraction of ~20%. Note also the domain border in (*b*) (adapted from [30,42]). (*c*,*d*) Diamond-type photonic crystals in the wing scales of the diamond weevil, *E. imperialis*. Photonic crystals are arranged in large domains with a chitin filling fraction of 35 % (investigated in more details in **chapters 9,10**).

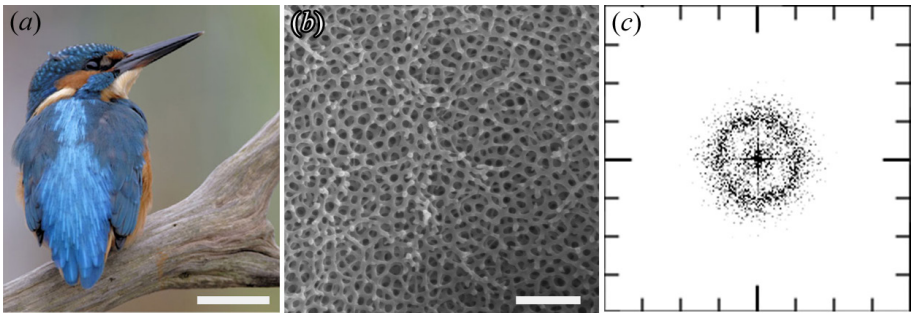

Figure 7: Quasi-ordered photonic structures. The blue-coloured feathers of the Common king fisher, *Alcedo atthis* (*a*), have quasi-ordered spongy keratin structures (*b*) that, when Fourier-transformed, show with a uni-modal feature size (*c*). Bars: (*a*) 5 cm, (*b*) 1 µm, (*c*) a unit distance represents a spatial frequency of 0.005 nm^{-1} = 5 μm^{-1} (see [45]).

1.2.4 Quasi-ordered photonic structures

Not only perfectly-ordered crystalline structures like those described above (figure 2) create structural colours. Also photonic structures with a local, short-range order, i.e. order on the nearest neighbour level, or disordered structures can produce structural coloration due to coherent light scattering. These structures are referred to as *quasi-ordered* photonic structures and can be characterised by an un-ordered distribution of local features (isotropy) that is represented by a ring-like pattern in the Fourier space (see figure 7c; ref. [44]).

Striking cases of quasi-ordered photonic structures can be - for example - found in disordered multilayer structures (see figure 1 of **Chapter 2**) or in the spongy photonic structures of many weevil scales and bird feathers [44-46], e.g. creating the blue coloration of parrots and kingfishers (see figure 7). Quasi-ordered structures also produce what is called non-iridescent colours since the colour of the surface does not change when the illumination and the viewing angle are changed simultaneously. However, the structures still feature strong iridescence when only one of the angles is altered [45].

1.3 Combination of pigmentary and structural coloration

So far, we have considered pigmentary and structural coloration individually, i.e. as disjunctive coloration mechanisms. In many animal integuments, however, pigmentary and structural colouration is often found simultaneously. The combination of pigmentary and structural coloration can lead to a number of optical effects: from an increase in either the optical contrast or the chromatic contrast of the overall reflectance, to adjusting the spectral shape of the (unaltered) photonic structure. In the following, these three mechanisms will be presented in more detail.

1.3.1 Increasing the optical contrast

The presence of broad-band absorbing pigmented tissue, e.g. melanised tissue, below the photonic structure enhances the saturation of the colour signal reflected by the photonic structure, since stray light and light at wavelengths outside the photonic bandgaps is effectively absorbed (figure 8a). Famous examples of animals employing this combination of pigmentary and structural coloration are butterflies of the genus *Morpho*, where melanised ground scales are present below the tree-shaped interference reflectors, resulting in the highly saturated blue colour of the butterflies [1,47].

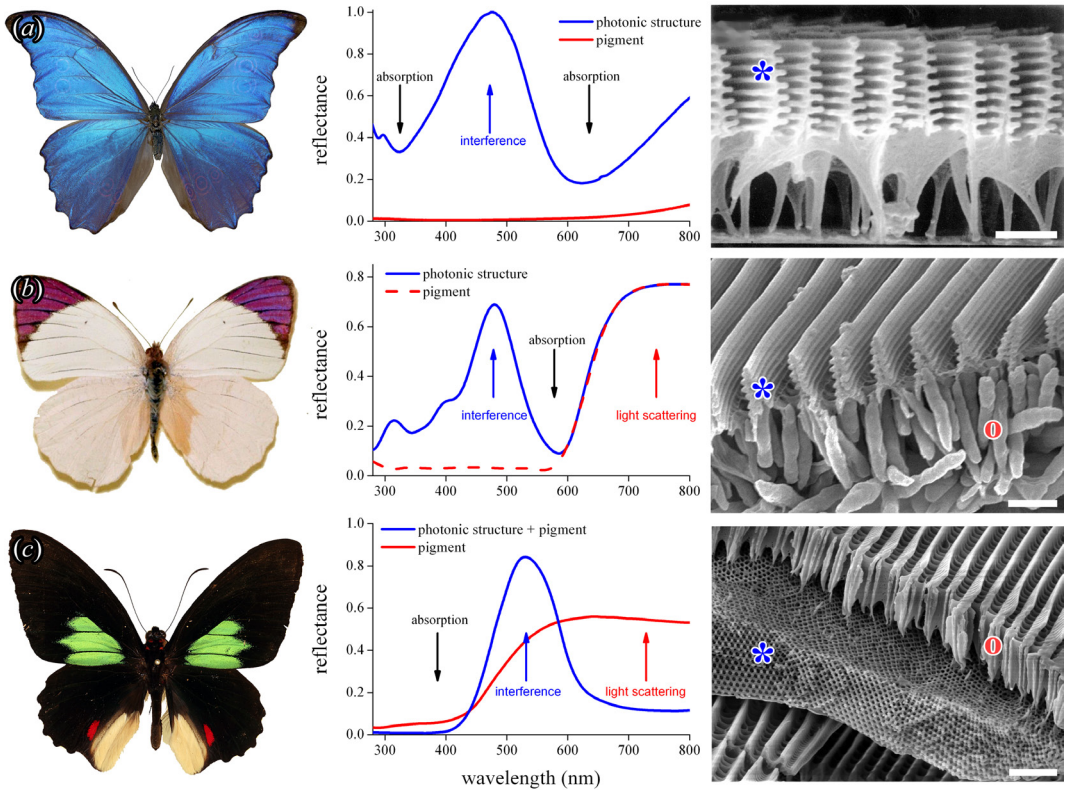

Figure 8: Examples of the combination of structural and pigmentary colouration.
(*a*) Increasing the optical contrast: *Morpho* butterflies enhance the brilliancy of the photonic structure (blue star) by a melanin layer below the blue-reflecting scales that absorbs possible straylight. (*b*) Increasing the chromatic contrast: pierid butterflies, here *Colotis regina*, have narrow-band absorbing pigment filters concentrated in granules (red circle) below the interference reflectors (blue star). (*c*) Spectral tuning: in *Parides sesostris*, a pigment filter (red circle) tunes the structural coloration (blue star) by absorbing light in the UV-wavelength range (see **Chapter 8**). Scale bars: (a-c) 1 µm.

1.3.2 Increasing the chromatic contrast

The presence of diffusing, narrow-band absorbing tissue, instead of a broad-band absorbing tissue, below the photonic structure has two optical consequences. The pigmented tissue firstly acts as an effective stray light absorber, similar to the case of broad-band absorbers above. Secondly, the scattering of non-absorbed light additionally increases the spectral fullness of the reflected signal (see figure 8b) and thus increases the chromatic contrast.

This combination is frequently found in pierid butterflies, where UV- or blue-reflecting interference reflectors are paired with narrow-band absorbing pterin pigments that are packed in disordered granules below the photonic structure. The resulting visual signal has two components: a static, diffusive component due to pigmentary coloration and a dynamic, directed component due to reflectance from the interference reflector. This chromatic and dynamic colour signal potentially acts as a mate recognition signal [16,18].

1.3.3 Spectral tuning

In the aforementioned cases, the absorbing pigment is situated below the photonic structure. In cases where the absorbing substance is part of the photonic structure or situated above it,

the pigmented tissue changes the photonic properties of the nanostructured material such that it acts as an optical filter on the reflectance spectrum (see figure 8c).

In **Chapters 6 & 7,** we investigate the multilayered photonic structure of various papilionid butterflies of the *nireus* group in which a pigment filter suppresses the iridescence and creates an angle-independent wing pattern.

In **Chapter 8**, we show that a UV- and blue-absorbing pigment filters the reflectance of randomly oriented single-network gyroid-type photonic crystal in the wing scales of the Emerald-patched Cattleheart, *Parides sesostris***.** Therefore, the reflectance of the photonic crystals that is originally ranging from the UV to the green wavelength range is restricted to the green wavelength range.

2. Biological Relevance of animal coloration

Light is a significant and important selection pressure for the evolution of animals, having ultimately led to the astonishing diversity in the spectacular displays of many animals that we encounter today. From a functional perspective, animal coloration appears to be important in a multitude of ways, since animals often actively use their integuments for display purposes, e.g. in intra- and interspecific communication (see figure 9, refs. [3,4,14]).

Organismal body colours can serve for agonistic behaviour between males of the same species, for instance in territorial defence, or generally as a visually obvious criterion for sexual selection, e.g. by signalling fitness or territorial strength, or to warn potential predators. Body coloration can, however, also provide cryptic camouflage in a foliaceous background, so to avoid predation by fading in with the background. Furthermore, the presence of nanostructured materials may strengthen tissues or increase the hydrophobicity of the surface and thus also fulfil non-communicative functions.

Technically, pigmentary and structural colours serve the same primary tasks since they are both subsets of general animal coloration. When compared to pigmentary colour signalling, structural colours have *unique* properties: they are (usually) directional and bright, have a narrow spectral reflectance and they are iridescent, i.e. they change colour with a change in the viewing geometry. Therefore, photonic structures may be seen as *specialised* forms of visual communication devices in that they often fulfil a particular biological function in display; e.g. by maximizing conspicuousness to conspecifics, by selectively enhancing light reflectance of a certain polarisation.

When discussing possible biological functions of animal coloration, we always have to keep in mind that the visual system of animals is different from our own in a number of ways. For example, the visual spectral range is different: while the spectral range is ~400-750 nm for humans, insects can also detect UV light, i.e. their spectral range covers ~300-700 nm. This implies, that e.g. the colour of the Cabbage white butterfly, *Pieris rapae*, although white for us appears ‘butterfly-yellow’ to conspecifics due to absorption in the UV wavelength range. Furthermore, the visual system of insects allows detection of polarisation signals and thus opens a ‘secret’ communication channel that cannot be detected by predators (or by humans).

In this section, we will present some of the most important biological aspects of animal coloration for the photonic structures presented in this thesis. More complete overviews of the possible biological functions of animal coloration can be found elsewhere [14,48].

2.1 Sex recognition and mate choice

An obvious function of coloration is sex recognition, especially since many animals show a strong sexual dichromatism, i.e. the coloration of males and females of the same species differ. In most butterflies, for example, mostly the males of a species exhibit iridescent coloration, whereas females are coloured solely by pigments. Therefore, to achieve recognition by mates, a unique optical signature has to be displayed by the animal and conspecifics must be able to recognize members of their own species by the coloration and/or changes thereof.

An often discussed communication channel is UV coloration, based on iridescent colours. Well-studied examples are pierid butterflies that show strong variations in their optical signature, i.e. the UV-coloration and the present pigment, within a number of (closely related) butterflies [16].

But also polarised light offers an important sex recognition channel. In two *Heliconius* butterflies, it has been shown that potential mates are recognised by their (presence and lack of) polarised iridescence [49]. In **Chapter 4,** we investigate the metallic elytra of *C. fulgidissima* and show that light reflected by the elytra is strongly polarised under high incidence angles, thus presumably serving as a mate recognition signal.

The colourful displays further play a role in mate choice. In studies with UV-reflecting pierid butterflies, males with a higher UV reflectance had a higher copulation success than males

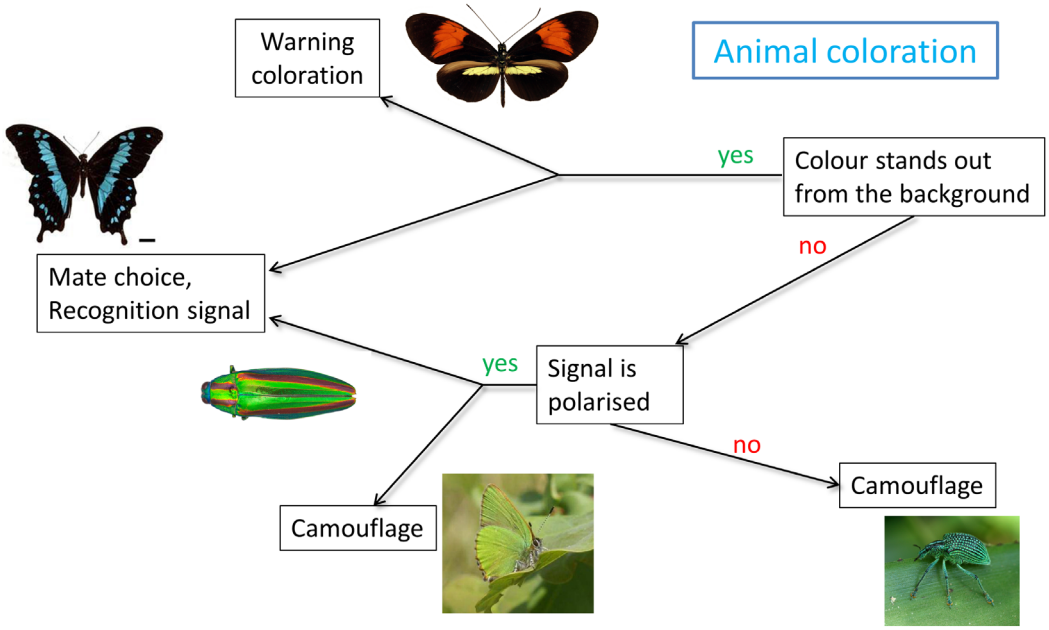

Figure 9: Flowchart showing the possible functions of animal coloration. Representative animals for each category discussed in the text are shown next to the connected functions. Double arrows indicate a possible double function.

with a lower UV signal [50]. Similarly, the number of iridescent eye spots in the peacock tail feather appears to be important for the mating success [51]. An intriguing question is whether the visual system of the animals has undergone convergent evolution with the (iridescent) coloration it displays. This interesting aspect has as yet to be investigated in detail. In **Chapter 5**, we investigate the seductively shiny occipital feathers of a bird of paradise, Lawes's parotia, and discuss the specific role of the silvery feathers in the courtship display.

2.2 Warning coloration

Coloration is often used to warn predators of the potential un-palatability and toxicity of the potential prey [52], e.g. by displaying special wing patterns. This so-called *aposematic* or *warning* coloration, once evolved, gives rise to colour mimicry of toxic species by non-toxic conspecifics, leading to convergent evolution of specific coloration patterns in mimicry rings [53]. A particularly well-studied example is the genus *Heliconius*, where a number of mimicry rings can be observed [54].

In **Chapter 8**, we elucidate the coloration mechanism of the Neotropical butterfly *Parides sesostris* that displays a striking green wing coloration as an aposematic display to potential predators [35,52].

2.3 Camouflage

Camouflage is not a true communication channel, rather the opposite, since coloration that permits camouflage has the purpose of *avoiding* detection by predators rather than enhancing visiblity to mates. In the animal kingdom, there are a number of ways to avoid predation by camouflage. The most common way of camouflaging is by fading in with the background of the habitat, i.e. by adapting its spectral properties.

The Green Hairstreak, *Callophrys rubi*, has randomly ordered domains of gyroid-type photonic crystals in its wing scales. Light reflected by the scales blends together diffusely and so creates a dull greenish coloration that matches with the foliaceous background (see figure 6a, refs. [30,42]). Interestingly, the reflected light from *C. rubi* is circularly polarised for certain wavelengths and may also be used as a mate recognition signal while simultaneously functioning as cryptic camouflage [30,34]. Whether or not the polarised signal can be observed by conspecific butterflies still has to be investigated. Similarly, the camouflage of some cephalopods with polarised signals may offer a 'secret' communication channel for conspecifics [55].

In **Chapter 10,** we investigate the structural-coloured wing scales on the diamond weevil, *Entimus imperialis*, which are arranged inside concave pits. We show that this special scale arrangement provides a two-fold biological function related to the distance of the observer: from close up, the shininess of the elytra facilitates intersexual recognition; from far away, the weevil merges with a foliaceous background, thus providing cryptic camouflage.

3. References

1. Kinoshita, S. 2008 *Structural colors in the realm of nature*. Singapore: World Scientific.
2. Parker, A. R. 2005 A geological history of reflecting optics. *J. R. Soc. Interface* **2**, 1-17.
3. Vukusic, P. & Sambles, J. R. 2003 Photonic structures in biology. *Nature* **424**, 852-855.

4. Biró, L. P. & Vigneron, J. 2011 Photonic nanoarchitectures in butterflies and beetles: valuable sources for bioinspiration. *Laser Photon. Rev.* **5**, 27-51.
5. Joannopoulos, J. D. 2008 *Photonic crystals: molding the flow of light*, 2nd edn. Princeton: Princeton University Press.
6. Whitney, H. M., Kolle, M., Andrew, P., Chittka, L., Steiner, U. & Glover, B. J. 2009 Floral iridescence, produced by diffractive optics, acts as a cue for animal pollinators. *Science* **323**, 130-133.
7. Snow, M. & Pring, A. 2005 The mineralogical microstructure of shells: Part 2. The iridescence colors of abalone shells. *Am. Mineral.* **90**, 1705-1711.
8. Parker, A. R. & Townley, H. E. 2007 Biomimetics of photonic nanostructures. *Nat. Nanotechnol.* **2**, 347-353.
9. Guldin, S., Huttner, S., Kolle, M., Welland, M. E., Muller-Buschbaum, P., Friend, R. H., Steiner, U. & Tetreault, N. 2010 Dye-sensitized solar cell based on a three-dimensional photonic crystal. *Nano Lett.* **10**, 2303-2309.
10. Chutinan, A., John, S. & Toader, O. 2003 Diffractionless flow of light in all-optical microchips. *Phys. Rev. Lett.* **90**, 123901.
11. Pris, A. D., Utturkar, Y., Surman, C., Morris, W. G., Vert, A., Zalyubovskiy, S., Deng, T., Ghiradella, H. T. & Potyrailo, R. A. 2012 Towards high-speed imaging of infrared photons with bio-inspired nanoarchitectures. *Nat. Photon.* **6**, 195-200.
12. Potyrailo, R. A., Ghiradella, H., Vertiatchikh, A., Dovidenko, K., Cournoyer, J. R. & Olson, E. 2007 *Morpho* butterfly wing scales demonstrate highly selective vapour response. *Nat. Photon.* **1**, 123-128.
13. Kolle, M., Salgard-Cunha, P. M., Scherer, M. R., Huang, F., Vukusic, P., Mahajan, S., Baumberg, J. J. & Steiner, U. 2010 Mimicking the colourful wing scale structure of the *Papilio blumei* butterfly. *Nat. Nanotechnol.* **5**, 511-515.
14. Doucet, S. M. & Meadows, M. G. 2009 Iridescence: a functional perspective. *J. R. Soc. Interface* **6 Suppl 2**, S115-S132.
15. Stavenga, D. G., Stowe, S., Siebke, K., Zeil, J. & Arikawa, K. 2004 Butterfly wing colours: scale beads make white pierid wings brighter. *Proc. R. Soc. B* **271**, 1577-1584.
16. Wilts, B. D., Pirih, P. & Stavenga, D. G. 2011 Spectral reflectance properties of iridescent pierid butterfly wings. *J. Comp. Physiol. A* **197**, 693-702.
17. Wijnen, B., Leertouwer, H. L. & Stavenga, D. G. 2007 Colors and pterin pigmentation of pierid butterfly wings. *J. Insect Physiol.* **53**, 1206-1217.
18. Giraldo, M. A. 2008 *Butterfly wing scales: pigmentation and structural properties*. Groningen: PhD Thesis.
19. Yoshioka, S. & Kinoshita, S. 2007 Polarization-sensitive color mixing in the wing of the Madagascan sunset moth. *Opt. Express* **15**, 2691-2701.
20. Wilts, B. D., Leertouwer, H. L. & Stavenga, D. G. 2009 Imaging scatterometry and microspectrophotometry of lycaenid butterfly wing scales with perforated multilayers. *J. R. Soc. Interface* **6**, S185-S192.
21. Stavenga, D. G., Matsushita, A., Arikawa, K., Leertouwer, H. L. & Wilts, B. D. 2012 Glass scales on the wing of the swordtail butterfly *Graphium sarpedon* act as thin film polarizing reflectors. *J. Exp. Biol.* **215**, 657-662.
22. Bálint, Z., Kertész, K., Piszter, G., Vértesy, Z. & Biró, L. P. 2012 The well-tuned blues: the role of structural colours as optical signals in the species recognition of a local butterfly fauna (Lepidoptera: Lycaenidae: Polyommatinae). *J. R. Soc. Interface* **9**, 1745-1756.
23. Hariyama, T., Hironaka, M., Takaku, Y., Horiguchi, H. & Stavenga, D. G. 2005 The leaf beetle, the jewel beetle, and the damselfly; insects with a multilayered show case. In *Structural color in biological systems - principles and applications* (eds. S. Kinoshita & S. Yoshioka), pp. 153-176. Osaka: Osaka University Press.
24. Stavenga, D. G., Wilts, B. D., Leertouwer, H. L. & Hariyama, T. 2011 Polarized iridescence of the multilayered elytra of the Japanese Jewel Beetle, *Chrysochroa fulgidissima. Phil. Trans. R. Soc. B.* **366**, 709-723.
25. Yeh, P. 2005 *Optical waves in layered media*. Hoboken NJ: Wiley-Interscience.
26. Zi, J., Yu, X., Li, Y., Hu, X., Xu, C., Wang, X., Liu, X. & Fu, R. 2003 Coloration strategies in peacock feathers. *Proc. Natl. Acad. Sci. U. S. A.* **100**, 12576-12578.
27. Welch, V., Vigneron, J. P., Lousse, V. & Parker, A. 2006 Optical properties of the iridescent organ of the comb-jellyfish *Beroe cucumis* (Ctenophora). *Phys. Rev. E* **73**, 041916.
28. Welch, V. L., Vigneron, J. P. & Parker, A. R. 2005 The cause of colouration in the ctenophore *Beroe cucumis. Curr. Biol.* **15**, R985-6.

29. Trzeciak, T. M. & Vukusic, P. 2009 Photonic crystal fiber in the polychaete worm Pherusa sp. *Phys. Rev. E* **80**, 061908.
30. Michielsen, K. & Stavenga, D. G. 2008 Gyroid cuticular structures in butterfly wing scales: biological photonic crystals. *J. R. Soc. Interface* **5**, 85-94.
31. Leertouwer, H. L., Wilts, B. D. & Stavenga, D. G. 2011 Refractive index and dispersion of butterfly chitin and bird keratin measured by polarizing interference microscopy. *Opt. Express* **19**, 24061-24066.
32. Hyde, S., Andersson, S., Larsson, K., Blum, Z., Landh, T., Lidin, S. & Ninham, B. 1997 *The Language of shape: the role of curvature in condensed matter: physics, chemistry, and biology*. Amsterdam: Elsevier.
33. Hyde, S. T. & Schröder-Turk, G. E. 2012 Geometry of interfaces: topological complexity in biology and materials. *Interface Focus* **2**, 529-538.
34. Saba, M., Thiel, M., Turner, M. D., Hyde, S. T., Gu, M., Grosse-Brauckmann, K., Neshev, D. N., Mecke, K. & Schröder-Turk, G. E. 2011 Circular dichroism in biological photonic crystals and cubic chiral nets. *Phys. Rev. Lett.* **106**, 103902.
35. Wilts, B. D., Michielsen, K., De Raedt, H. & Stavenga, D. G. 2012 Iridescence and spectral filtering of the gyroid-type photonic crystals in *Parides sesostris* wing scales. *Interface Focus* **2**, 681-687.
36. Saranathan, V., Osuji, C. O., Mochrie, S. G., Noh, H., Narayanan, S., Sandy, A., Dufresne, E. R. & Prum, R. O. 2010 Structure, function, and self-assembly of single network gyroid ($I4_132$) photonic crystals in butterfly wing scales. *Proc. Natl. Acad. Sci. U. S. A.* **107**, 11676-11681.
37. Poladian, L., Wickham, S., Lee, K. & Large, M. C. 2009 Iridescence from photonic crystals and its suppression in butterfly scales. *J. R. Soc. Interface* **6 Suppl 2**, S233-S242.
38. Seago, A. E., Brady, P., Vigneron, J. P. & Schultz, T. D. 2009 Gold bugs and beyond: a review of iridescence and structural colour mechanisms in beetles (Coleoptera). *J. R. Soc. Interface* **6 Suppl 2**, S165-84.
39. Wilts, B. D., Michielsen, K., De Raedt, H. & Stavenga, D. G. 2012 Hemispherical Brillouin zone imaging of a diamond-type biological photonic crystal. *J. R. Soc. Interface* **9**, 1609-1614.
40. Galusha, J. W., Richey, L. R., Gardner, J. S., Cha, J. N. & Bartl, M. H. 2008 Discovery of a diamond-based photonic crystal structure in beetle scales. *Phys. Rev. E* **77**, 050904.
41. Ghiradella, H. 1994 Structure of butterfly scales: patterning in an insect cuticle. *Microsc. Res. Tech.* **27**, 429-438.
42. Michielsen, K., De Raedt, H. & Stavenga, D. G. 2010 Reflectivity of the gyroid biophotonic crystals in the ventral wing scales of the Green Hairstreak butterfly, *Callophrys rubi*. *J. R. Soc. Interface* **7**, 765-771.
43. Joannopoulos, J. D., Meade, R. D. & Winn, J. N. 1995 *Photonic crystals*: Princeton University Press.
44. Saranathan, V., Forster, J. D., Noh, H., Liew, S., Mochrie, S. G. J., Cao, H., Dufresne, E. R. & Prum, R. O. 2012 Structure and optical function of amorphous photonic nanostructures from avian feather barbs: a comparative small angle X-ray scattering (SAXS) analysis of 230 bird species. *J. R. Soc. Interface* **9**, 2563-2580.
45. Stavenga, D. G., Tinbergen, J., Leertouwer, H. L. & Wilts, B. D. 2011 Kingfisher feathers - colouration by pigments, spongy nanostructures and thin films. *J. Exp. Biol.* **214**, 3960-3967.
46. Pouya, C., Stavenga, D. G. & Vukusic, P. 2011 Discovery of ordered and quasi-ordered photonic crystal structures in the scales of the beetle *Eupholus magnificus*. *Opt. Express* **19**, 11355-11364.
47. Yoshioka, S. & Kinoshita, S. 2006 Structural or pigmentary? Origin of the distinctive white stripe on the blue wing of a *Morpho* butterfly. *Proc. R. Soc. B* **273**, 129-134.
48. Andersson, M. 1994 *Sexual selection*. Princeton, NJ.: Princeton University Press.
49. Sweeney, A., Jiggens, C. & Johnsen, S. 2003 Polarized light as a butterfly mating signal. *Nature* **423**, 31-32.
50. Kemp, D. J. 2008 Female mating biases for bright ultraviolet iridescence in the butterfly *Eurema hecabe* (Pieridae). *Behav. Ecol.* **19**, 1-8.
51. Loyau, A., Gomez, D., Moureau, B., Thery, M., Hart, N. S., Saint Jalme, M., Bennett, A. T. D. & Sorci, G. 2007 Iridescent structurally based coloration of eyespots correlates with mating success in the peacock. *Behav. Ecol.* **18**, 1123-1131.
52. Pinheiro, C. E. G. 1996 Palatability and escaping ability in Neotropical butterflies: Tests with wild kingbirds (*Tyrannus melancholicus*, Tyrannidae). *Biol. J. Linn. Soc.* **59**, 351-365.
53. Mallet, J. 2010 Shift happens! Shifting balance and the evolution of diversity in warning colour and mimicry. *Ecol. Entomol.* **35**, 90-104.
54. Hines, H. M., Counterman, B. A., Papa, R., Albuquerque de Moura, P., Cardoso, M. Z., Linares, M., Mallet, J., Reed, R. D., Jiggins, C. D., Kronforst, M. R. & McMillan, W. O. 2011 Wing patterning gene redefines the mimetic history of *Heliconius* butterflies. *Proc Natl Acad Sci U S A* **108**, 19666-19671.
55. Mäthger, L. M. & Hanlon, R. T. 2006 Anatomical basis for camouflaged polarized light communication in squid. *Biol. Lett.* **2**, 494-496.